Zeitschrift: IABSE congress report = Rapport du congrès AIPC = IVBH Kongressbericht

Band: 12 (1984)

Artikel: System damping effects on cable-stayed bridges

Autor: Maeda, Ken-ichi / Yoneda, Masahiro / Maeda, Yukio

DOI: https://doi.org/10.5169/seals-12193

System Damping Effects on Cable-Stayed Bridges

Vibration et amortissement des ponts haubannés

Systemdämpfungseffekte von Schrägseilbrücken

Ken-ichi MAEDA
Dr. Eng.
Kawada Industries
Tokyo, Japan

Ken-ichi Maeda, born in 1949, got his Dr. Eng. in 1984 at Osaka University. His major field of activity is long-span bridge engineering. He is at present manager of the Research Laboratory, Kawada Industries, Inc.

Masahiro YONEDA
Res. Eng.
Kawada Industries
Tokyo, Japan

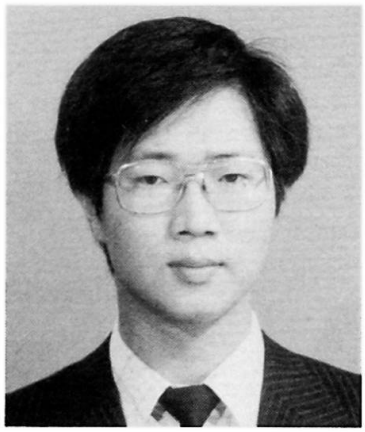

Masahiro Yoneda, born in 1954, got his M. Eng. in 1980 at Kanazawa University. His major field of activity is wind effects on structures. He is employed at the Research Laboratory, Kawada Industries, Inc.

Yukio MAEDA
Prof. Dr.
Osaka University
Osaka, Japan

Yukio Maeda, born in 1922, got his B.E. at Hokkaido University and Dr. Eng. at University of Tokyo. Since 1969 he is Professor of Structural Engineering, Osaka University. At present he is Vice Chairman of Technical Committee, IABSE.

SUMMARY

For the purpose of obtaining basic data on wind resistant design, wind-induced characteristic responses with system damping effects on cable-stayed bridges are studied. The causes of the system damping are defined, and an analytical technique involving time series response using results of a sectional model wind tunnel test is proposed. Then, from an actual bridge test and an analysis of an actual design example, general features are discussed.

RESUME

Dans le but d'obtenir les charges statiques et dynamiques du vent, nécessaires au dimensionnement des ponts suspendus, on étudie les réponses dynamiques du système. Ces réponses dynamiques et leur amortissement ont été étudiées de manière analytique, sur modèles en soufflerie et in situ.

ZUSAMMENFASSUNG

Um grundlegende Daten für die Bemessung auf Wind zu erhalten, werden die charakteristischen Reaktionen unter Windbelastung anhand der Systemdämpfungseffekte von Schrägseilbrücken untersucht. Die wichtigsten Ursachen der Systemdämpfung werden definiert und ein analytisches Verfahren, bei dem die Ergebnisse aus einem Modellversuch im Windkanal verwendet werden, wird vorgeschlagen und anhand eines Versuchs an einer Brücke erörtert.

1. INTRODUCTION

The system damping effect which would prevent bending oscillations of cable-stayed bridges and secure hereby their dynamic safety, was first pointed out by F. Leonhardt[1]. However, judging from the results of full-scale measurements of several bridges built in Japan, the system damping effect cannot be considered as characteristics common to all of the cable-stayed bridges. Namely, it seems that the governing cause and real response are not completely clarified yet, and the development of analytical study is indispensable as well as further actual bridge tests. Because the effects on wind-induced responses, principally observed at a few actual bridge tests and during the construction, are difficult to be directly examined by full-model wind-tunnel tests. Consequently, there are many problems remaining unsolved, and the application to a design has not been generally carried out yet.

In these circumstances, the purpose of the present study is to obtain basic data on the application of the effects of system damping to a wind resistant design. In this paper, first, by investigating the behaviour of so-called internal resonance, the authors define governing causes of the system damping of cable-stayed bridges. Then, the authors treat bending aeolian oscillations among various kinds of wind-induced responses, and propose an analytical technique of time series response using unsteady aerodynamic forces given by a sectional model wind-tunnel test, taking into consideration the internal resonance. Next, the validity of the definition and the analytical technique is confirmed by an actual bridge test. Moreover, the time series response analysis of an actual design example is performed using the results of a spring-mounted model test. Finally, the authors attempt to conclude general features of the present study.

2. DEFINITION OF GOVERNING CAUSES

In this chapter, the authors define that the function of staying cables as a damped absorber[2] in Fig.1 (tuned mass damper in a wide sense) and the beating phenomena (from another angle, a main girder and particular cables exchange their oscillation energy) are governing causes of the system damping of cable-stayed bridges, when so-called internal resonance in terms of bending oscillations of a main girder and of transverse local oscillations of cables remarkably occurs. The defined causes are examined by using a solution of a complex eigenvalue problem concerning a simple simulation model of cable-stayed bridges.

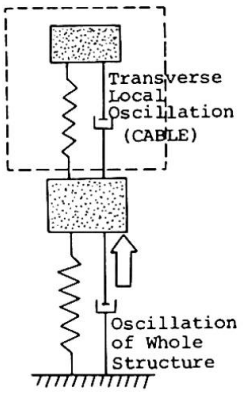

Fig.1 Damped absorber

Fig.2 shows the simulation model with 2-degree of freedom for a study on the defined causes. The equation of free damping oscillation may be given as follows :

$$\begin{bmatrix} m_g+m_c/2 & 0 \\ 0 & m_c \end{bmatrix}\begin{bmatrix} \ddot{x}_g \\ \ddot{x}_c \end{bmatrix}+\begin{bmatrix} c_g & 0 \\ 0 & c_c \end{bmatrix}\begin{bmatrix} \dot{x}_g \\ \dot{x}_c \end{bmatrix}+\begin{bmatrix} k_{gg} & k_{gc} \\ k_{gc} & k_{cc} \end{bmatrix}\begin{bmatrix} x_g \\ x_c \end{bmatrix}=\begin{bmatrix} 0 \\ 0 \end{bmatrix} \quad (1)$$

where $\ddot{x}$, $\dot{x}$, x, m, c and k express the acceleration, the velocity, the displacement, the mass, the structural damping coefficients and the stiffness, respectively. And suffix g or c indicates the values of a girder or a cable, respectively.

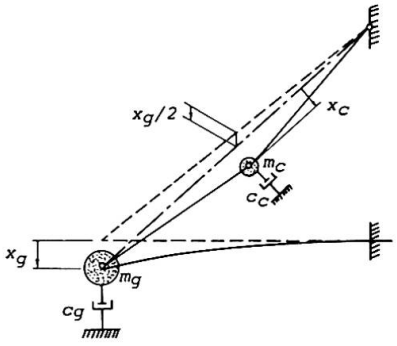

Fig.2 Simulation model

If a model as shown in Fig.3, in which the transverse oscillation of the cable is neglected, and another model with only the transverse oscillation of the cable in Fig.4 are presumed here, the equations of motion is respectively given from Eq.(1) as follows :

$$(m_g+m_c/2)\ddot{x}_g+c_g\dot{x}_g+k_{gg}x_g=0 \quad \cdots\cdots\cdots\cdots (2)$$

$$m_c\ddot{x}_c+c_c\dot{x}_c+k_{cc}x_c=0 \quad \cdots\cdots\cdots\cdots (3)$$

Then, when ω_g and ω_c, h_g and h_c are respectively the natural circular frequencies and the structural damping constants of the models with 1-degree of freedom, the following equations are obtained :

$$\left.\begin{aligned} c_g &= 2(m_g+m_c/2)h_g\omega_g \\ k_{gg} &= (m_g+m_c/2)\omega_g^2 \end{aligned}\right\} \cdots\cdots (4) \qquad \left.\begin{aligned} c_c &= 2m_c h_c \omega_c \\ k_{cc} &= m_c\omega_c^2 \end{aligned}\right\} \cdots\cdots (5)$$

As an extreme case where the internal resonance occurs, the assumption $\omega_g=\omega_c=\bar{\omega}$ is made here. Thus, by substituting Eq.(4), Eq.(5) and the equations $x_g=X_g e^{i\Omega t}$, $x_c=X_c e^{i\Omega t}$, as a conventional approach, into Eq.(1), the following equation is obtained :

$$e^{i\Omega t}\begin{bmatrix} -\Omega^2+2ih_g\bar{\omega}\Omega+\bar{\omega}^2 & k_{gc}/(m_g+m_c/2) \\ k_{gc}/m_c & -\Omega^2+2ih_c\bar{\omega}\Omega+\bar{\omega}^2 \end{bmatrix}\begin{bmatrix} x_g \\ x_c \end{bmatrix}=\begin{bmatrix} 0 \\ 0 \end{bmatrix} \cdots\cdots (6)$$

From the condition of existence of significant solution of the above equation, two sets of the conjugate complex roots, Ω_1 and Ω_2, can be approximately derived as follows :

$$\left.\begin{aligned} \Omega_1 &\fallingdotseq i\{(h_g+h_c)/2\}\bar{\omega}\pm\sqrt{\bar{\omega}^2[1-\{(h_g+h_c)/2\}^2]-\alpha} \\ \Omega_2 &\fallingdotseq i\{(h_g+h_c)/2\}\bar{\omega}\pm\sqrt{\bar{\omega}^2[1-\{(h_g+h_c)/2\}^2]+\alpha} \end{aligned}\right\} \cdots\cdots (7)$$

where $\alpha=\{k_{gc}/(m_g+m_c/2)\}(k_{gc}/m_c)$. Moreover, the normalized natural modes, $\{\Phi_1\}$ and $\{\Phi_2\}$, can be obtained from Eq.(6) as follows :

$$\{\Phi_1\}=[\sqrt{1/\{2(m_g+m_c/2)\}},\ -\sqrt{1/(2m_c)}]^T,\quad \{\Phi_2\}=[\sqrt{1/\{2(m_g+m_c/2)\}},\ +\sqrt{1/(2m_c)}]^T \cdots\cdots (8)$$

Hence, by paying attention to bending aeolian oscillations due to wind forces acting on the girder, the following equation may be expressed for each time step:

$$\{\Phi_1\}^T[F_I]\{\Phi_1\}=\{\Phi_2\}^T[F_I]\{\Phi_2\}=\frac{1}{2}(\{\Phi_g\}^T[F_I]\{\Phi_g\}) \cdots\cdots (9)$$

where $[F_I]$ is the unsteady aerodynamic damping matrix which will be described in the next chapter, and $\{\Phi_g\}=[\sqrt{1/(m_g+m_c/2)},\ 0\ ]$ is the normalized mode when the transverse oscillations of the cable are neglected.

Therefore, it will be known that the bending oscillations due to wind forces acting on the girder are produced by two kinds of similarly coupled natural modes, $\{\Phi_1\}$ and $\{\Phi_2\}$, which are excited almost at the same time by means of the natural circular frequencies, $\omega_1=\sqrt{\bar{\omega}^2-\alpha}$ and $\omega_2=\sqrt{\bar{\omega}^2+\alpha}$, close to each other. Furthermore, it will be known that the following conditions can be easily satisfied, and that the total damping constant to each mode is increased as compared with the case where the internal resonance hardly occurs :

$$2\{(h_g+h_c)/2\}\omega_1-h_g^*/2 > 2h_g\omega_g-h_g^*,\quad 2\{(h_g+h_c)/2\}\omega_2-h_g^*/2 > 2h_g\omega_g-h_g^* \cdots\cdots (10)$$

where $h_g^*=\{\Phi_g\}^T[F_I]\{\Phi_g\}$. Also, it will be apparently known that beating phenomena remarkably occur, and amplitudes of the girder are periodically decreased, but without expending the energy. Consequently, it can be judged that the defined causes will be governing factors of the system damping of cable-stayed bridges.

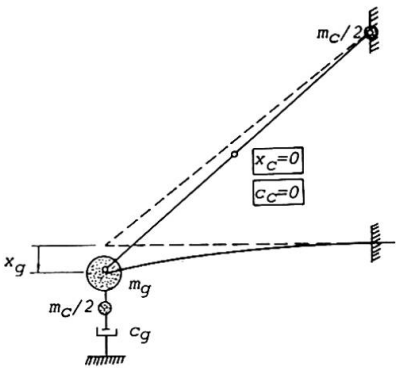

Fig.3 Model($x_c=0$)

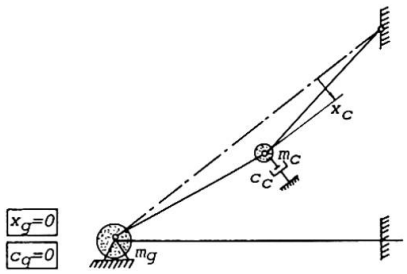

Fig.4 Model($x_g=0$)

3. ANALYTICAL TECHNIQUE USING RESULTS OF WIND-TUNNEL TEST

In this chapter, the authors deal with bending aeolian oscillations among various kinds of wind-induced responses, and propose an analytical technique of time series response using unsteady aerodynamic forces given by a sectional model wind-tunnel test, taking into consideration the internal resonance. Because, the system damping effect on cable-stayed bridges is difficult to be directly examined by full-model wind-tunnel tests.

To an analytical model of cable-stayed bridges with cables replaced by links for

considering their transverse local oscillations, the linearized equations of motion[3] may be given on the basis of the several assumptions as follows :

$$[M]\{\ddot{y}\}+[C]\{\dot{y}\}+[K]\{y\}=[F_I]\{\dot{y}\} \quad \cdots\cdots(11)$$

where $[M]$ is the mass matrix, and $[K]$ is the tangential stiffness matrix in a static equilibrium state. Also, $[C]$ is the structural damping matrix, and $[F_I]$ is the unsteady aerodynamic damping matrix. By performing the natural vibration analysis for the equation $[M]\{\ddot{y}\}+[K]\{y\}=\{0\}$, two kinds of similarly coupled natural modes of i-th and j-th orders, $\{\Phi_i\}$ and $\{\Phi_j\}$, and the natural circular frequencies close to each other, ω_i and ω_j, can be obtained when the internal resonance remarkably occurs. Moreover, if the normalization $\{\Phi_K\}^T[M]\{\Phi_K\}=1 \ (k=i,j)$ has been performed, Eq.(11) can be transformed into the following 2nd order differential equation relative to the generalized coordinates, q_i and q_j :

$$\ddot{q}_k+(2h_k\omega_k-\{\Phi_k\}^T[F_I]\{\Phi_k\})\dot{q}_k+\omega_k^2 q_k=0 \quad (k=i,j) \quad \cdots\cdots(12)$$

where h_i and h_j are the structural damping constants. But, being different from the conventional cases where only one kind of natural modes is considered, values assumed in a wind-tunnel test cannot be used as these constants. Also, these constants must be evaluated by taking account of degree of the internal resonance.

When h_g and h_c, ω_g and ω_c, $[C_g]$ and $[C_c]$, and $\{\Phi_g\}$ and $\{\Phi_c\}$ respectively express the structural damping constants, the natural circular frequencies, the damping matrices, and the normalized natural modes of the model neglecting transverse local oscillations of cables and also of the model for only transverse oscillations of cables, the following equations can be constituted :

$$2h_k\omega_k=\{\Phi_k\}^T[C]\{\Phi_k\}=\left[\{\Phi_{k,g}\}^T,\ \{\Phi_{k,c}\}^T\right]\begin{bmatrix}[C_g], & [0]\\ [0], & [C_c]\end{bmatrix}\begin{Bmatrix}\{\Phi_{k,g}\}\\ \{\Phi_{k,c}\}\end{Bmatrix} \quad (k=i,j) \quad \cdots\cdots(13)$$

$$2h_g\omega_g=\{\Phi_g\}^T[C_g]\{\Phi_g\}, \qquad 2h_c\omega_c=\{\Phi_c\}^T[C_c]\{\Phi_c\}$$

where $\{\Phi_{k,c}\}$ expresses only the transverse local oscillation component of the cables in $\{\Phi_k\}$, and $\{\Phi_{k,g}\}$ expresses $\{\Phi_k\}$ from which this component has been deducted. Thus, from the above equations and the fact that $\{\Phi_i\}$ and $\{\Phi_j\}$ are similar to each other, it seems that these values, h_i and h_j, may be evaluated by the following approximate expression :

$$2h_k\omega_k\fallingdotseq 2h_g\omega_g(\{\Phi_{k,g}\}^T\{\Phi_{k,g}\})/(\{\Phi_g\}^T\{\Phi_g\})+2h_c\omega_c(\{\Phi_{k,c}\}^T\{\Phi_{k,c}\})/(\{\Phi_c\}^T\{\Phi_c\}) \quad (k=i,j) \quad (14)$$

The validity of evaluating the structural damping constants by Eq.(14) will be confirmed in the next chapter.

Hence, by giving the matrix $[F_I]$, Eq.(12) can be expressed definitely. This matrix can be calculated by using the unsteady aerodynamic lift coefficient C_{LZI} obtained from the sectional model wind-tunnel test with the dimensionless amplitude Z_r and the reduced wind velocity U_r at each angle of attack. However, differently from the conventional cases, it is required to give U_r and Z_r corresponding to two kinds of natural circular frequencies close to each other and similarly coupled natural modes. These values may be computed as follows. Namely, the value of U_r may be given corresponding to the average value $(\omega_i+\omega_j)/2$ of the frequencies. On the other hand, the value of Z_r may be given corresponding to the equivalent amplitude vector $\{Z_p\}$ which can be expressed by the following equation in each time step :

$$\{Z_p\}=\sqrt{(q_i\{\Phi_i\}+q_j\{\Phi_j\})^2+\left(\frac{\dot{q}_i\{\Phi_i\}+\dot{q}_j\{\Phi_j\}}{(\omega_i+\omega_j)/2}\right)^2} \quad \cdots\cdots(15)$$

Therefore, by integrating Eq.(12) in succession with a small interval and applying the mode superposition method, the time series response analysis of bending aeolian oscillations can be performed taking into consideration the internal resonance. Furthermore, the proposed analytical technique can be easily extended to other kinds of wind-induced oscillations.

4. EXAMPLE OF FULL-SCALE MEASUREMENT

In this chapter, in order to confirm the validity of the defined causes and of evaluating the structural damping constants by using Eq.(14), the results of an actual cable-stayed PC bridge test are introduced and examined.

The bridge tested is as illustrated in Fig.5, in which it was anticipated at the time of design that the internal resonance would occur under completed conditions after grouting of HiAm-anchor cables. The tests conducted were a dropping load test and a moving load test. The weight, dropping position and moving speed of a loading car were about 2.0 t , the midpoint of the span and 30km/h, respectively. For the sake of comparison, the dropping test was made not only after grouting, but also before the grouting.

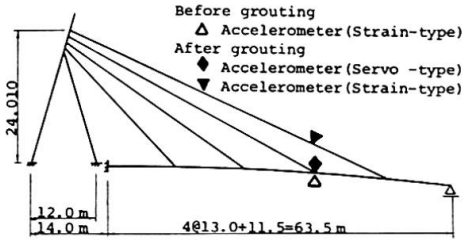

Fig.5 Cable-stayed PC bridge

Fig.6 shows the computed results of natural circular frequencies and modes together with the measured values. Fig.7 and Fig.8 show the recorded waveforms of the respective items of measurement at the dropping and moving load tests, respectively. Moreover, Table 1 shows the calculated values of damping constants by substituting the reasonable values, h_g=0.00477 and h_c=0.00637, into Eq.(14), corresponding to the measured values of logarithmic decrement, δ_g=0.03 and δ_c=0.04.

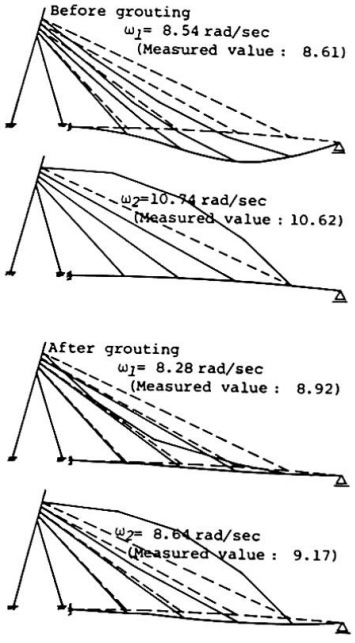

Fig.6 Natural circular frequencies and modes

Hence, it will be seen from Fig.6 that after the grouting, unlike before the grouting, two kinds of similarly coupled modes having close frequencies to each other exist apparently due to the internal resonance. Also, it will be seen from Fig.7 and Fig.8 that in the case of residual free oscillations after the grouting, amplitudes of the main girder are rapidly decreased, and that changes in the amplitude apparently due to the beating phenomenon are observed.

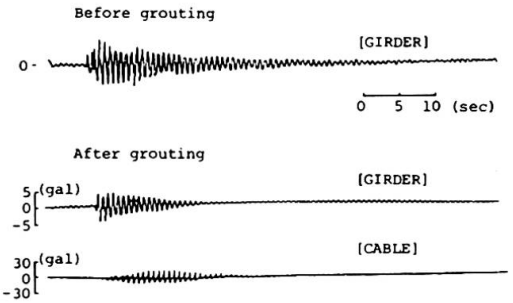

Fig.7 Dropping load test

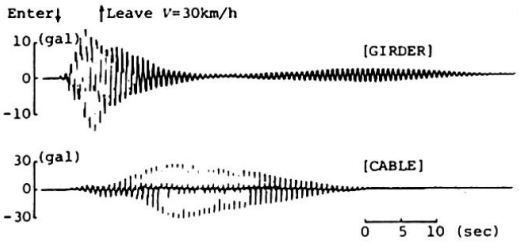

Fig.8 Moving load test

	ORDER	MODE	CALCULATED V. (δ_g=0.03, δ_c=0.04)	
Before grout.	1st	OSCILLATION OF GIRDER	δ_1	0.030
			h_1	0.00477
	2nd	OSCILLATION OF CABLE	δ_2	0.040
			h_2	0.00637
After grout.	1st	COUPLED OSCILLATION OF GIRDER AND CABLE	δ_1	0.037
			h_1	0.00589
	2nd		δ_2	0.033
			h_2	0.00525

Table 1 Damping constants

While, from Table 1, it will be known that the values of h_1 and h_2 corresponding to the coupled natural modes after the grouting are larger than the value of h_g. Also, it will be known that the sum of h_1 and h_2 after the grouting is equal to the sum of h_g and h_c, and that before the grouting, the value of h_1 corresponding to the non-coupled mode of the main girder is equal to the value of h_g.

Therefore, from the above considerations, it may be maintained that in actual bridges, the system damping due to the defined causes can occurs actually. The actual bridge for the test has satisfied the required conditions for the internal resonance incidentally in the design, and in case of multi-cable-stayed bridges,

possibilities of satisfying the conditions would have been higher. Thus, the defined causes may be considered to be a governing factor of the system damping experienced in the past. Furthermore, it may be considered that evaluation of the damping constant by Eq.(14) is appropriate, as one of the features of the proposed analytical technique.

5. TIME SERIES RESPONSE ANALYSIS FROM SPRING-MOUNTED MODEL TEST

In this chapter, a time series response analysis of bending aeolian oscillations with respect to an actual design example are performed using unsteady aerodynamic coefficients obtained from a spring-mounted model test. Then, it will be tried to obtain basic data for a wind resistant design related to the system damping effects of cable-stayed bridges.

5.1 Calculation Model Corresponding to Actual Design Problem

An actual design example to be considered is a multi-cable-stayed bridge[4] as shown in Fig.9 and Table 2. In the original design, this bridge has not satisfied the required conditions of the internal resonance. Thus, an additional mass is considered here corresponding to an actual problem for a comparison with the static design.

Consequently, in the case of this bridge with HiAm-anchor cables, by increasing the thickness of grouting, four kinds of calculation models are used here, in which characteristics of cables at the 10th and 11th levels are given as shown in Table 3.

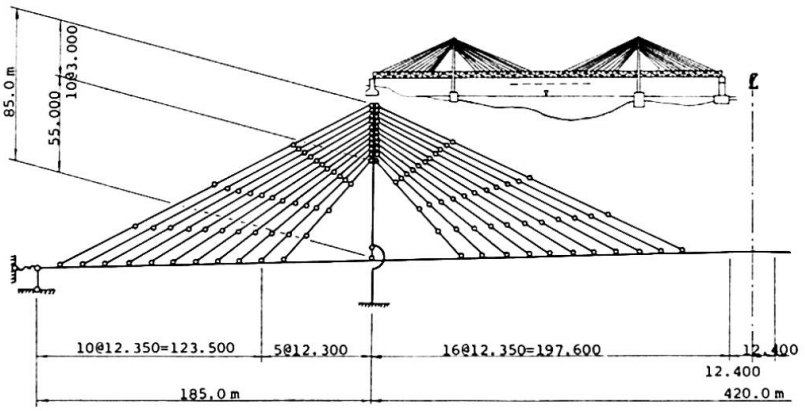

Fig.9 Skeleton

	AREA (m^2)	INERTIA (m^4)	Y.MODULUS (t/m^2)
GIRDER	1.0635 ~ 1.5747	40.538 ~ 65.585	21000000.0
TOWER	1.4780 ~ 2.2520	4.568 ~ 9.054	21000000.0
CABLE	0.0225 ~ 0.0419	0.0	20500000.0
SPRING (length : 3.0 m)	1.0	0.0	36000.0

Table 2 Sectional values

CABLE		MODEL	SECTIONAL VALUES AREA (m^2)	LENGTH (m)	DENSITY (t/m^3)	TOTAL WEIGHT (t)	NO. OF φ7mm - WIRE	PE - PIPE OUTSIDE DIAMETER	PE - PIPE WEIGHT (kg/m)	REQUIRED VALUE OF GROUT AREA (cm^2)	REQUIRED VALUE OF GROUT WEIGHT (kg/m)	REQUIRED VALUE OF GROUT DENSITY (t/m^3)	CIRCULAR FREQUENCY (rad/sec)
CENTER SPAN	10th	*MODEL-1,-1L*	0.03586	179.554	11.0	70.827	(117×4) ×2	φ125mm	15.04	474.54	76.913	1.62	3.324
		MODEL-2L											
		MODEL-3L			18.282	117.714		φ200mm	37.36	1781.83	315.723	1.77	2.578
	11th	*MODEL-1,-1L*	0.03586	191.907	11.0	75.700	(117×4) ×2	φ125mm	15.04	474.54	76.913	1.62	3.128
		MODEL-2L			16.192	111.430		φ180mm	30.72	1372.09	247.417	1.80	2.578
		MODEL-3L											
SIDE SPAN	10th	*MODEL-1,-1L*	0.04186	180.791	11.0	83.247	(136×4) ×2	φ140mm	18.56	632.85	109.458	1.73	3.097
		MODEL-2L											
		MODEL-3L			15.873	120.125		φ200mm	37.36	1725.15	294.690	1.71	2.578
	11th	*MODEL-1,-1L*	0.04186	193.208	11.0	88.965	(136×4) ×2	φ140mm	18.56	632.85	109.458	1.73	2.910
		MODEL-2L			14.025	113.429		φ180mm	30.72	1315.42	223.918	1.70	2.578
		MODEL-3L											

Table 3 Characteristics of HiAm-anchor cables

Namely, *MODEL-1* and *MODEL-1L* correspond to the cases where transverse local oscillations of the cables are neglected and considered without adjusting distributed

mass, respectively. *MODEL-2L* corresponds to the case where the requirements for the internal resonance are satisfied by adding a mass to the four uppermost cables at the 11th level. *MODEL-3L* corresponds to the case where the same adjustment is made to four cables at 10th level in addition to the 11th level.

5.2 Natural Oscillation Characteristics

The natural circular frequencies and modes concerning the 1st order symmetric oscillation of the main girder are shown in Fig.10. Namely, the mode superposition method is applied by paying attention to the modes shown in this figure. However, in *MODEL-1L*, the mode of the 10th order is apparently not excited by the unsteady aerodynamic forces acting on the main girder, but is indicated there as reference.

5.3 Structural Damping Constants

By considering four cases of h_C, the values of structural damping constants h_i and h_j corresponding to each mode evaluated by Eq.(14) are used, namely, for *CASE-1*, *CASE-2*, *CASE-3* and *CASE-4*, in which a value of 0.03 is used as the logarithmic decrement $\delta_g=2\pi h_g$, the values of $\delta_C=2\pi h_C$ are varied from 0.0 to 0.0075, to 0.0150 and to 0.0300, respectively.

5.4 Unsteady Aerodynamic Force

As the unsteady aerodynamic lift coefficient C_{LZI}, a value is applied corresponding to the reduced wind verocity U_r=1.992 shown in Fig.11, which is formulated by the least square method by using V-A-δ curve (wind velocity-amplitude-logarithmic decrement curve)[5] obtained from the results of a wind-tunnel test of the spring-mounted model in the case of an angle of attack of 5-degrees. For reference, ratio of C_{LZI} to dimensionless amplitude $z_r=z_0/B$ is also shown in Fig.11.

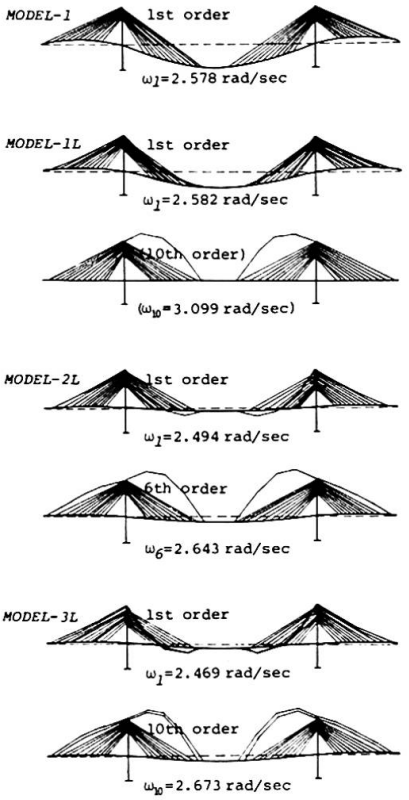

Fig.10 Natural circular frequencies and modes

5.5 Results and Consideration

A part of calculated results of the time series response analysis is shown in Fig.12, when the initial value of vertical displacement amplitude at 1/2 point of the main girder is 0.150 m.

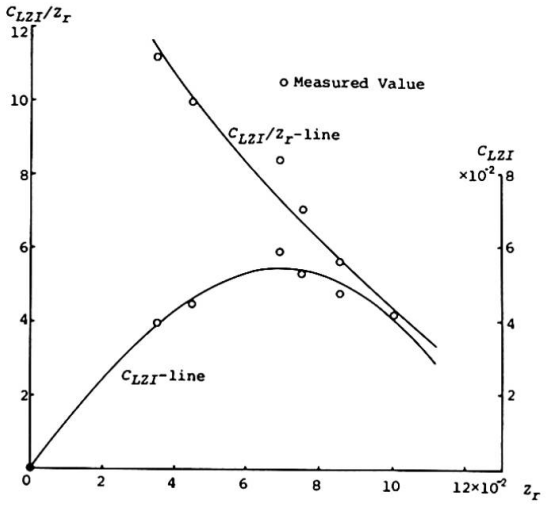

Fig.11 Unsteady aerodynamic force

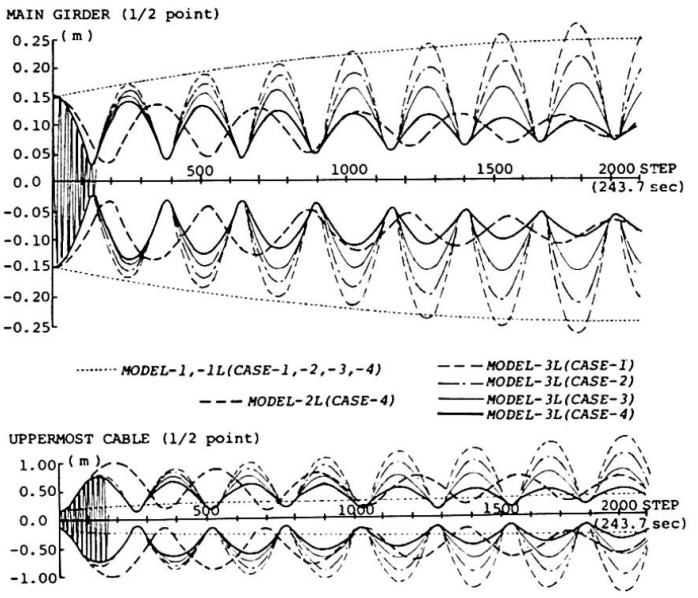

Fig.12 Amplitudes to steady state

This figure shows an envelope of the response amplitudes from the initial development stage to the steady state of vertical displacements at 1/2 points of the main girder and the uppermost cable of the center span. From this figure, it will be known that there is almost no difference between *MODEL-1* and *MODEL-1L*, and that, in the case of *MODEL-2L* and *MODEL-3L*, the amplitude is gradually decreased periodically. Moreover, in the case of *MODEL-3L*, it will be known that the steady state amplitude slightly increases in *CASE-1* where the function of the cable as a damped absorber is neglected, but becomes considerably small in *CASE-2* and *CASE-3* compared to *MODEL-1L*. Also, it will be known that, in *CASE-4*, the development of oscillations is even restricted in the case of *MODEL-2L* and *MODEL-3L*.

6. CONCLUSIONS

From the afore-mentioned discussions, the following conclusions may be drawn :

(1) It can be judged that the defined causes are governing factors of the system damping of cable-stayed bridges, which are the function of staying cables as a damped absorber (tuned mass damper in a wide sense) and the beating phenomena when the internal resonance in terms of bending oscillations of a main girder and of transverse local oscillations of cables remarkably occurs.

(2) By enhancing the action of cables as a damped absorber by using materials with higher damping capacity, it is not difficult to even restrict the occurrence of wind-induced oscillation of main girders of cable-stayed bridges by means of the system damping effect.

(3) It is positively predictable that the examination of the system damping effect due to the defined causes will become not negligible in the wind resistant design of cable-stayed bridges. Especially, by satisfying the requirements for the internal resonance by adjusting a distributed mass of particular cable of multi-cable-stayed bridges, the system damping effect enables to considerably reduce steady state amplitudes and are effective for improving the aerodynamic stability without an impediment to the static design.

(4) For the examination of the system damping, the proposed analytical technique of time series response taking into consideration the internal resonance is appropriate, which is easily extended to other kinds of wind-induced oscillations by using results of sectional model wind-tunnel tests.

Finally, the authors would like to express the deepest appreciation to Prof. M. Ito (University of Tokyo), to Prof. Y. Ohchi (Hosei University) and to Dr. H. Yamaguchi (Saitama University) for their valuable advices during the present study, and also to Mr. M. Yasuda and Dr. S. Narui (Honshu-Shikoku Bridge Authority) for their valuable data given to the authors.

REFERENCES

1) Leonhardt, F. et al. : Cable-Stayed Bridges, IABSE SURVEYS, S-13/80, 1980.

2) Den Hartog, J.P. : Mechanical Vibrations, 4th Edition, McGraw-Hill Book Inc., 1956.

3) Y. Kubo, M. Ito and T. Miyata : Nonlinear Analysis of Aerodynamic Response of Suspension Bridges in Wind, Proc. of JSCE, No.252, 1976 (in Japanese).

4) Japan Society of Civil Engineers : Report of Technical Research and Study on 'Hitsuishijima-Bashi' and 'Iwagurojima-Bashi' Cable-Stayed Bridges, Part III, 1980 (in Japanese).

5) Honshu-Shikoku-Bridge Authority : Report of Wind-Tunnel Tests for Main Truss Girder of 'Iwagurojima-Bashi' Cable-Stayed Bridge, Part II, 1980 (in Japanese).